2022-10-13

Rheological and Physicochemical Analysis of Nonedible Oils Used for Biodiesel Production

Zakaria, Francisca

ACS Omega

https://doi.org/10.1021/acsomega.2c02960

ACS OMEGA

http://pubs.acs.org/journal/acsodf

Article

Rheological and Physicochemical Analysis of Nonedible Oils Used for Biodiesel Production

Francisca Zakaria, Frank Lujaji, and Thomas Kivevele*

Cite This: *ACS Omega* 2022, 7, 37133−37141

Read Online

ACCESS | Metrics & More | Article Recommendations

ABSTRACT: Rheological and physicochemical characteristics of edible oils used for biodiesel production are well established; nonetheless, the rheological and physicochemical characteristics of nonedible oils are yet to be established. The present study therefore focuses on rheological and physicochemical characterization of nonedible vegetable oils that can be used as biodiesel feedstock. The selected vegetable oils studied include cashew nut shell liquid (CNSL), castor oil (CO), *Croton megalocarpus* oil (CMO), *Podocarpus usambarensis* oil (PUO), and *Thevetia peruviana* oil (TPO). Physicochemical parameters analyzed were free fatty acids, acid value, saponification value, peroxide value, iodine value, specific gravity, and moisture content using methods by the Association of Official Analytical Chemists (AOAC). Rheological properties were analyzed using a VT-550 Thermo Haake Viscotester operated by the Rheowin 3 Job Manager software. The preset parameters in the Viscotester were shear rate and temperature. The shear rate increased uniformly from 5 to 100 s^{-1} at the temperature range of 30−60 °C. The experimental data were fitted into rheological models of Newton, Bingham, Ostwald−de Waele (power-law), and Herschel−Bulkley using Rheowin 3 Data Manager. The oil yield was 29−65%, highlighting the feedstock's potential for commercial biodiesel production. At a constant temperature, all oil samples exhibited a Newtonian flow behavior. In contrast to edible oils, nonedible oils exhibited high shear stress, emphasizing the reconstruction of new appropriate designs of production systems. The rheological models appropriate to represent the flow behavior of the samples were the Newton and Ostwald−de Waele models, with a fit of R^2 = 0.990−1.000.

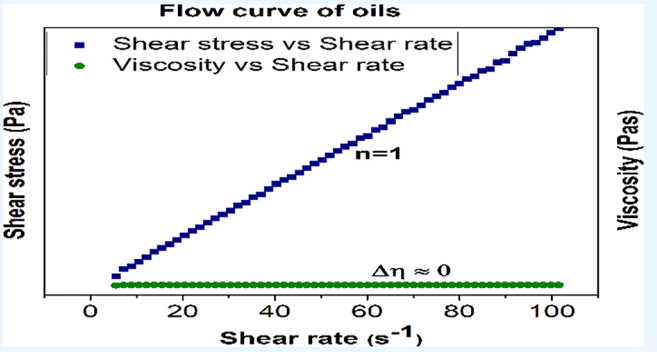

1. INTRODUCTION

Biodiesel is produced by the transesterification process that converts oils and fats into biodiesel (methyl esters) and glycerine.[1] The characteristics of biodiesel produced are dependent on the physicochemical and rheological characteristics of the feedstock used during the manufacturing process.[2] The performance and quality of biodiesel fundamentally depend on the chemical, structural, and flow properties of the vegetable feedstock oil used.[3] Generally, biodiesel is characterized by higher density, higher viscosity, and lower volatility than mineral diesel, affecting steady fuel exhaustion.[4] This preceding nature of biodiesel is based on the influence of the feedstock vegetable oils' physical behavior and chemical composition.[3] Vegetable oils are characterized by larger hydrocarbon chains of triglycerides (free fatty acids), and the fuel quality, stability, and conversion efficiency are compromised.[5] Furthermore, free fatty acids influence the other physicochemical properties of the fuel including but not limited to the saponification value, iodine value, and peroxide value. Therefore, even though the biodiesel industry is fast-growing, the maintenance of fuel quality and stability remains an unsolved impediment.[6] To address the challenge, physicochemical and thermophysical characteristics of the feedstock were studied for the designation of the process control systems and appropriate manufacturing facilities, storage facilities, and transportation facilities. A study[7] emphasized the importance of analyzing the physicochemical and rheological characteristics of the raw materials of biodiesel.

Rheology is the study of the flow behavior of fluids and the effect of applied stress on the fluids.[4] It provides the information to be used in the designation of the manufacturing facilities, storage facilities, and process control systems based on the flow behavior of the feedstock.[4] A study by Silva et al.[4] focused primarily on the rheology of the first-generation (edible vegetable oils) biodiesel feedstock at 35, 45, and 60 °C. To the best of the authors' knowledge, there is no study that

Received: May 12, 2022
Accepted: September 29, 2022
Published: October 13, 2022

comprehensively reported the rheology behavior of non-vegetable oils as feedstock for biodiesel production. This study, therefore, aims to characterize second-generation feedstock (nonedible vegetable oils) that could be used as biodiesel feedstock. The flow behavior analysis of the selected vegetable oils was conducted at 30−60 °C. The selected nonedible oils used in this research were cashew nut shell liquid (CNSL), castor oil (CO), *Croton megalocarpus* oil (CMO), *Podocarpus usambarensis* oil (PUO), and *Thevetia peruviana* oil (TPO). The studied nonedible vegetable oils were selected based on the oil yield and the reproduction term (the life span) of the seed-bearing plant. The reported yield was 20−30% for CNSL,[8,9] 35−45% for CMO,[10] 28−59% for CO,[11] and 50−67% oil yield for PUO and TPO.[12,13] The average reproductive term starts after 6−18 months for CNSL, CO, and TPO; 4 years for CMO; and 15 years for PUO. The reproductive term for the seed-bearing plants lasted 45 years for PUO and CMO, 3 years for CO, 50 years for CSNL, and 75 years for TPO.

2. MATERIALS AND METHODS

2.1. Materials and Chemicals. The cashew nut shell liquid (CNSL) was obtained from Korosho Africa Limited, a local cashew nut processing factory in Tunduru district, Southern East Tanzania. Castor oil (CO) was obtained from the local small seed processing industry in Dodoma, central Tanzania. *Croton megalocarpus* oil (CMO), *Podocarpus usambarensis* oil (PUO), and *Thevetia peruviana* oil (TPO) were extracted from the seeds collected from various regions of the country.

Croton megalocarpus and *Podocarpus usambarensis* seeds were purchased from Tanzania Forest Service Agency (TFSA). The seeds were collected from Usambara forests in Lushoto, Tanga, in the Northern East part of Tanzania. *Thevetia peruviana* seeds were collected from the outskirts of Arusha and Kilimanjaro regions in the northern part of Tanzania. Shown in Figure 1 are the seeds before the removal of the shells and the oil extraction process.

Reagents used as solvents for oil extraction were analytical-grade petroleum ether and chloroform. For physicochemical characterization of the samples, chemicals used were analytical-grade petroleum ether, ethanol, POP indicator, potassium hydroxide, hydrochloric acid, glacial acetic acid, chloroform, potassium iodide, starch indicator, sodium thiosulfate, carbon tetrachloride, and Wiji's solution. The reagents were bought from Exodus Chemicals and Apparatus Trading (ECAT) in Arusha CBD.

Figure 1. The seeds from which the feedstock oil was extracted: (A) cashew nut shells, (B) castor seeds, (C) *Croton megalocarpus* seeds, (D) *Podocarpus usambarensis* seeds, and (E) *Thevetia peruviana* seeds.

2.2. Sample Preparation. The shells of the seeds were removed and separated from the kernels. The kernels were washed, sun dried for 12 h, and crushed to 2−5 mm particles. Except for the cashew nut shells, the oil samples were extracted from the kernels of the seeds.

2.3. Oil Extraction. Oil from CMO, PUO, and TPO was extracted from the crushed kernels of the seeds by employing the solvent extraction method.[14,15] The petroleum ether was used to extract *Croton megalocarpus* oil and *Podocarpus usambarensis* oil from the seeds.[13,16] Chloroform was used to extract *Thevetia peruviana* oil from the seeds.[17] Solvent selection for oil extraction depends on the affinity of the solvent for a specific oil.[18,19] All the sample oils from CNSL, CO, CMO, PUO, and TPO were used for physicochemical and rheological characterization with no further treatment.

2.4. Physicochemical Characterization of the Samples. The techniques followed in determining the physicochemical parameters are summarized in Table 1. Physicochemical parameters of the oil samples were studied using the methods by the Association of Official Analytical Chemists (AOAC).

Table 1. Physicochemical Characterization Techniques[a]

parameter	method	principle
oil yield		gravimetry
FFA	AOAC 940.28	titrimetry
AV	AOAC 940.28	titrimetry
SV	AOAC 920.160	titrimetry
PV	AOAC 965.33	titrimetry
IV	AOAC 920.159	Wiji's titrimetry
SG	AOAC 920.212	pycnometry
moisture content	AOAC 930.15	gravimetry

[a]FFA = free fatty acid, AV = acid value, SV = saponification value, PV = peroxide value, IV = iodine value, and SG = specific gravity.

2.5. Investigation of Rheological Characteristics of Oils. Flow properties of the samples were analyzed by a shear rheometer (Haake Viscotester, model VT 550, Karlsruhe, Germany). This research used a concentric cylinder measuring system (CC MS) employing Searle's operating method for the experiments. The measuring system entailed a stationary outer cylinder mounted on the same axis as the rotating inner cylinder (sensor system).

The gap between the outer and inner cylinder was filled with the sample to be analyzed. To ensure a uniform stress distribution on the sample between the concentric cylinders, the degree of heterogeneity of stresses $\left(\varepsilon = \frac{R_c}{R_r}\right)$ for the setup was 1.084. The literature by Mezger[20,21] and Schramm[22] recommended that the ratio of the outer cylinder to that of the inner cylinder be at least a unit to get accurate measurements.

As the inner cylinder was in rotation, adequate torque to subdue the sample's viscosity, posing resistance to the induced motion, was measured. Rheological flow parameters that were analyzed in concurrence with the system fixtures and speed of inner cylinder (ω) are expressed as shown:

https://doi.org/10.1021/acsomega.2c02960
ACS Omega 2022, 7, 37133−37141

$$\gamma = \frac{2\omega R_c^2}{R_r^2 - R_c^2} \quad (1)$$

$$\tau = \frac{M}{2\pi R_r^2 L} \quad (2)$$

$$\eta = \frac{\tau}{\gamma} \quad (3)$$

In eqs 1−3, γ, τ, η, and M represent the shear rate (s^{-1}), shear stress (Pa), viscosity (Pa·s), and the torque measured (Nm), respectively.

System operation throughout the experiments was controlled by the Rheowin 3 Job Manager software. The rheometer was operated under controlled shear rate mode (CR), and the rheological characteristics of the samples were analyzed at 30, 40, 50, and 60 °C. The temperature was measured by a thermostatic sensor (Pt 100) coupled with the device. The shear rate was increased from 5 to 100 s^{-1} for 60 s for each experiment conducted. To ensure the precision of the results, experiments were carried out in triplicates using a fresh sample for each experiment. Rheological parameters were computed using the mean values of the replicates on Rheowin 3 Data Manager. The research focused on the relationship exhibited by the shear stress and viscosity parameters, with shear rate variation at the selected uniform temperature. Results presented in rheograms were fit into four rheological models to find the model that describes the rheological properties of the samples. Models selected to investigate the correlation among the parameters were Bingham, Herschel−Bulkley, Newton, and Ostwald−de Waele, also known as the power-law model. Mathematical expressions of the models are as follows:

Bingham:

$$\tau = \tau_o + \eta_p \gamma \quad (4)$$

Herschel−Bulkley:

$$\tau = \tau_o + K\gamma^n \quad (5)$$

Newton:

$$\tau = \eta\gamma \quad (6)$$

Ostwald−de Waele:

$$\tau = K\gamma^n \quad (7)$$

In eqs 4−7, τ represents the shear stress (Pa), γ represents the shear rate (s^{-1}), η represents the viscosity of the samples (Pa·s), τ_o represents the yield stress (Pa), η_p represents Bingham's plastic viscosity, K represents the consistency index (Pa·s^n), and n represents the flow behavior index (dimensionless).

The mathematical representation of Ostwald−de Waele's flow model can be reduced to Newton's model. Hence, the application of the Ostwald−de Waele flow model was to illustrate the relationship between the viscosity and the shear rate. Furthermore, the Bingham flow model was used to determine the yield stress necessary to start the flow by overcoming the viscous resistance of the samples. Therefore, fitting results into the models estimates the behavioral variations of the sample's parameters at the unmeasured shear rates.

3. RESULTS AND DISCUSSION

3.1. Proximate Analysis of the Seeds. As presented in Table 2, the proximate analysis of the selected seeds revealed that CS, CM, PU, and TP possessed a considerable amount of protein and fat compositions.[10,13,23,24] However, in CNS, there was a high fiber and oil composition.[25] The moisture content in CNS was also significant, which was attributed to the ability of the fiber to absorb moisture.[25] The fat composition of the seeds was used as a key determinant of a good biodiesel feedstock in this study.

Table 2. Proximate Composition of the Seeds[a]

constituents (%)	CNS	CS	CM	PU	TP
protein	3.8	28	41	17	26
fat	32	51	29	65	63
ash	10.6	9.4	3.5	2.3	2.2
carbohydrates	0.1	7.9	19	11	5.5
fiber	52	1.0	4.5	3.0	1.9
moisture	0.9	0.5	0.3	0.1	0.4

[a]CNS = cashew nut shell, CS = castor seeds, CM = *Croton megalocarpus*, PU = *Podocarpus usambarensis*, and TP = *Thevetia peruviana*.

3.2. Physicochemical Characteristics of Oils. Physicochemical characteristics of selected nonedible oils are summarized in Table 3. The FFA profile of feedstock oils determines the path taken in the biodiesel production process. The results showed that the FFA profile of CO, CMO, PUO, and TPO is <2%, suggesting that biodiesel synthesis from these oils can be achieved by a single-stage process.[26] The low composition of FFA in the samples showed that the sample oils were still fresh and of high quality. Conversely, the CNSL FFA profile is >2%, suggesting that the route for the biodiesel manufacturing process could be achieved through a double-stage process. The double-stage process requires excess alkali to neutralize the oil's acidity and also function as a catalyst. Excess alkali increases the yield of biodiesel by inhibiting soap formation that is usually due to the high FFA composition in the feedstock.[27] The high FFA composition in CNSL was due to the high moisture content in the sample oil.[28] The results revealed that the FFA composition of the selected vegetable oils correlated to other studies conducted in East Africa. A study by Kivevele and Mbarawa[29] and by Uwiragiye and Anyiam[30] stated that the FFA profile of CMO is 1.73 and 1.54%, respectively. Omari et al.[31] reported that the FFA profiles in CO from different regions of Tanzania varied from 0.22 to 0.99%. Saponification values ranged from 66.8 to 190.7

Table 3. Physicochemical Characteristics of the Selected Nonedible Oils

property	unit	CNSL	CO	CMO	PUO	TPO
FFA	%	6.6	0.9	1.61	1.2	0.96
AV	mgKOH/g	13.2	1.8	3.22	2.4	1.92
SV	mgKOH/g	66.8	183	190.7	190	120
PV	mequiv/kg	43.1	3.7	2.3	4.9	2.7
IV	mgI_2/100 g	124.4	82.8	126.5	96	83.1
SG		935	910	900	830	790
moisture content	%	5.53	0.05	1.1	0.01	0.03
oil yield	%			29	65	63

https://doi.org/10.1021/acsomega.2c02960
ACS Omega 2022, 7, 37133−37141

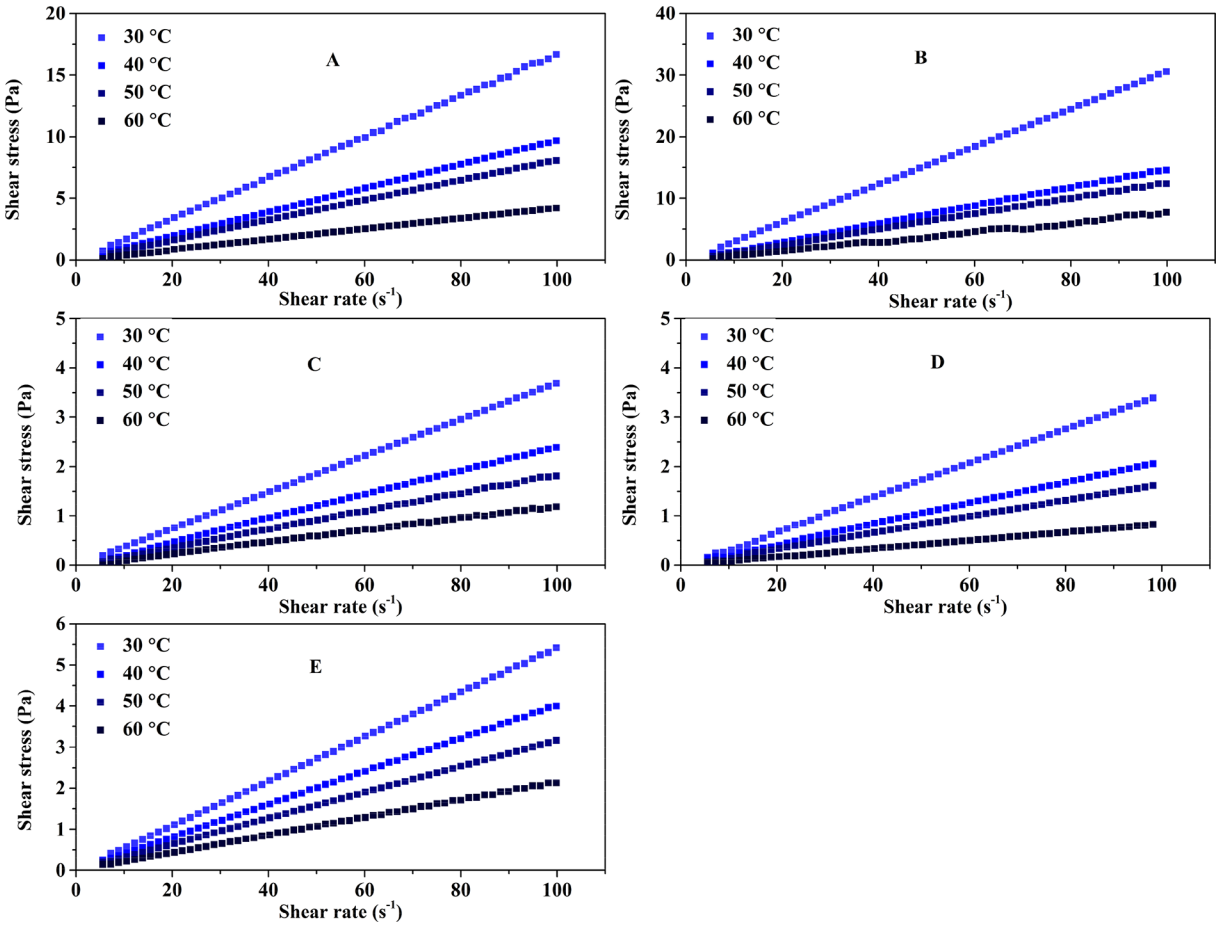

Figure 2. Flow curves of sample oils at the temperatures of 30, 40, 50, and 60 °C. (A) Cashew nut shell liquid, (B) castor oil, (C) *Croton megalocarpus* oil, (D) *Podocarpus usambarensis* oil, and (E) *Thevetia peruviana* oil.

mgKOH/g. As depicted in Table 3, the saponification values of CMO and PUO were 190.7 and 190 mgKOH/g, respectively, indicating a relative similarity. The resemblance of saponification values suggests that incorporated oil samples of CMO and PUO in this study were composed of carbon−carbon chains with the same molecular weight and carried similar functional groups. The similarity in saponification values resulted from the direct linkage between the saponification value and the molecular weight of the triglyceride chains (fatty acid chains) present in the oil. While all the other sample oils possessed saponification values that agree with the commended saponification values reported in the literature (such as Chavan et al., 2018;[32] Kyei et al., 2019;[9] Omari et al., 2015[31]), the observed value for PUO was slightly higher compared to the study by Minzangi et al.[13] The study reported that the saponification value of PUO extracted from the seeds collected in Kivu, DRC, was 182.5 mgKOH/g, and the deviation could be attributed to the differences of ecological habitat features such as the soil's primary nutrients, climatic conditions, and the altitude of the area where the plant was grown.[13] The mentioned factors influence the plant's nutrient uptake, causing minor variations in the properties of the oils. Also, the difference was possibly because of the chemical composition of impurities that were present in the sample oil.[30] However, not enough amount of research based on PUO has been conducted.

With the exception of CNSL, peroxide values of oils observed were <10 mequiv/kg, verifying that the samples used were still fresh. It also showed that it would take some time before the samples deteriorated. The peroxide value of CNSL was 43.1 mequiv/kg, relatively higher, which could be attributed to the oxidation reaction occurring during the oil extraction process, which involved roasting the shells.[25] Also, the high moisture content contributed to the oxidation of the liquid and resulted to a high peroxide value. The peroxide values of CO, CMO, PUO, and TPO were in sync with those reported in other literature. The iodine values recorded in this study were between 82.8 and 126.5 mgI_2/100 g. It was observed that CNSL and CMO had the highest iodine values of 124.4 and 126.5 mgI_2/100 g, respectively. The values suggested that the oil samples possessed a considerable amount of unsaturated fatty acids and had low oxidative stability characteristics.[33] A study by Shalaby[34] stated that nonedible oils were characterized by high iodine values and hence have low oxidative stability. Also, the iodine values of CNSL and CMO were comparatively similar, which could be accredited to an approximately equal number of unsaturated carbon−carbon bonds in the fatty acids. However, the value of CMO observed in this study was less than that observed by Kumar et al.,[35] which was 139.2 mgI_2/100 g. Similarly, the observed iodine value of CNSL was lower than the reported standard value of 250 mgI_2/100 g. The difference could be accounted for by thermo-oxidative alteration during the extraction process that caused the unsaturated carbon bonds of fatty acids to break.[36]

https://doi.org/10.1021/acsomega.2c02960
ACS Omega 2022, 7, 37133−37141

Table 4. Rheological Model's Parameters at 30 °C

	Newton $\tau = \eta\gamma$		Bingham $\tau = \tau_0 + \eta_p\gamma$			Ostwald–de Waele $\tau = K(\gamma)^n$			Herschel–Bulkley $\tau = \tau_0 + K(\gamma)^n$			
oils	η	R^2	τ_0	η_p	R^2	K	n	R^2	τ_0	K	n	R^2
CNSL	0.1604	0.999	−0.0646	0.1617	0.999	0.1729	0.980	0.999	−0.5611	0.2844	0.8741	0.996
CO	0.2949	0.999	−0.3427	0.2995	0.998	0.2769	1.014	0.999	−0.6765	0.3557	0.9643	1.000
CMO	0.0334	1.000	0.0000	0.0334	1.000	0.0335	1.000	1.000	−0.0001	0.0335	1.000	0.999
PUO	0.0340	0.992	−0.6760	0.0357	0.993	0.02219	1.070	0.993	−0.7259	0.0374	0.9927	0.993
TPO	0.0565	0.990	0.1322	0.0548	0.991	0.09427	0.996	0.993	−0.3703	0.1682	0.9985	0.994

Table 5. Rheological Models' Parameters at 40 °C

	Newton $\tau = \eta\gamma$		Bingham $\tau = \tau_0 + \eta_p\gamma$			Ostwald–de Waele $\tau = K(\gamma)^n$			Herschel–Bulkley $\tau = \tau_0 + K(\gamma)^n$			
oils	η	R^2	τ_0	η_p	R^2	K	n	R^2	τ_0	K	n	R^2
CNSL	0.09410	0.995	0.04774	0.0935	0.959	0.1381	0.991	0.997	−0.9445	0.3314	0.7412	0.998
CO	0.1336	0.999	−0.0652	0.1345	0.999	0.1234	1.018	1.000	0.0180	0.1215	1.021	0.978
CMO	0.01769	0.997	0.02865	0.0173	0.998	0.02508	0.9980	0.999	−0.0619	0.3533	0.8530	0.995
PUO	0.01749	1.000	−0.0005	0.0175	0.993	0.01747	1.000	1.000	−0.0012	0.0176	0.9985	0.993
TPO	0.03732	1.000	0.00956	0.0372	0.999	0.03937	0.9878	1.000	−0.0134	0.0410	0.9798	0.999

Table 6. Rheological Models' Parameters at 50 °C

	Newton $\tau = \eta\gamma$		Bingham $\tau = \tau_0 + \eta_p\gamma$			Ostwald–de Waele $\tau = K(\gamma)^n$			Herschel–Bulkley $\tau = \tau_0 + K(\gamma)^n$			
oils	η	R^2	τ_0	η_p	R^2	K	n	R^2	τ_0	K	n	R^2
CNSL	0.0733	0.999	−0.0348	0.0738	0.999	0.07218	1.004	0.999	−0.6423	0.1409	0.8759	1.000
CO	0.1101	0.999	−0.1040	0.1115	0.999	0.09724	1.028	1.000	−0.0378	0.1011	1.020	1.000
CMO	0.0236	0.987	−0.4059	0.0180	0.971	0.1003	0.999	0.990	−0.064	0.0034	1.086	0.929
PUO	0.0185	1.000	−0.0004	0.0185	1.000	0.01861	0.9999	1.000	−0.0004	0.0187	0.9985	0.934
TPO	0.0337	0.998	−0.0378	0.0344	0.983	0.02279	1.096	0.999	0.0728	0.0152	1.186	0.948

As reported on Table 3, the specific gravity values of oils were between 800 and 960. Specific gravity values of CNSL and CO samples were within the set standard range, which is 950–970 and 968–975.7 for the oils, respectively.[31,37] The moisture content in CO, CMO, PUO, and TPO was within the accepted standard range that was ≤0.05% for maintenance of the oil quality.[19,38] However, the moisture content in CNSL was 5.53%, which was extremely high considering the recommended standard value. The high moisture content in CNSL increased the rate of degradation of the oil.[9] The studies show that moisture content in biodiesel feedstock compromised the quality of the feedstock. Also, it affected the production efficiency of the oil because of soap formation during the process.[33,39] To resolve the drawbacks caused by the high moisture content of the feedstock, it is recommended for the oils to be dried to a moisture content of ≤0.05%. After extraction, the yield of vegetable oils was between 29 and 65%. CMSO had the lowest yield of only 29%, below the average range of 30–32% reported by Aliyu et al.[10] and Wu et al.[40] However, the yield was above the satisfactory range for biodiesel feedstock, which was at least 20% oil yield from the seeds.[41,42]

3.3. The Variation of Shear Stress and Dynamic Viscosity with Shear Rate. The internal resistance to flow offered by the selected raw materials that are used in the manufacturing process of biodiesel predetermines the flow behavior that is to be exhibited by the produced biodiesel.[43] Therefore, carrying out a thermophysical analysis of the feedstock in advance determines the suitable production processes and facilities designs.[4]Figure 2 presents the computed flow curves that show the shear rate–shear stress relationship of each oil sample at 30, 40, 50, and 60 °C. As shown in Figure 2, for all the samples analyzed, a uniform linear correlation of shear stress as a function of shear rate is revealed. For CNSL, CO, CMO, PUO, and TPO, the shear stress–shear rate flow relationship observed in this study was that of an ideal liquid that exhibits a Newtonian flow behavior. The results revealed that at zero shear rate, there was no minimum shear stress (y-intercept = 0 Pa) required to break the interactive bonds among the particles of the sample to start the flow of the sample oils. The shear rate applied to the samples was directly proportional to the shear stress exhibited by the samples for overcoming the viscous resistance offered. Because the rheograms illustrate that the sample oils possessed a Newtonian flow behavior, it implies that for each of the samples analyzed, the viscosity remained constant regardless of the increase in the shear rate applied. To further confirm the observed nature of the flow exhibited by the samples in the study, a linear fit on a power model was carried out to determine the behavior index of the samples.

$$\tau = K\gamma^n$$

$$\ln \tau = n\ln \gamma + \ln K \quad (8)$$

Equation 8 represents power-law as the equation of a straight line. The flow behavior index (n) represents the slope of the flow curves, and K is the consistency index representing the y-intercept.

The sample's flow behavior index categorizes the sample's flow into either Newtonian or non-Newtonian flow. The Newtonian flow was represented by a flow behavior index that equals 1. In contrast, the non-Newtonian flow is represented by a flow behavior index that can be either less than or greater than 1. According to the power model in Tables 3–6, the flow behavior index (n) of the linear fit was carried out for all the samples $0.9877 \leq n \geq 1.1000$. For all the computed values of n, there was an insignificant variation from the actual value of n

https://doi.org/10.1021/acsomega.2c02960
ACS Omega 2022, 7, 37133–37141

for substances that exhibit Newtonian flow, which is $n = 1$. Moreover, upon fitting the computed data in the respective model, the calculated correlation coefficient R^2 values for all the samples were greater than 0.99. This verified that the linearity of the flow curves and Newtonian flow behavior exhibited by the sample oils of the samples were appropriately represented by the power-law. A report by Wang et al.[44] that studied the rheological characteristics of CO observed a similar behavior. However, no rheological studies have been conducted for other selected vegetable oils used in this research. High values of shear stress were observed during the analysis of CNSL and CO samples because of the oils' high viscous resistance. The high viscosity of these samples is associated with strong intermolecular cohesive forces that resist the motion of the molecules. As a result, high torque is required to overcome the intermolecular force resistance for the flow to occur. The average viscosity of CNSL, CO, and TPO observed in this study was higher than the average viscosity of edible oils reported by Silva et al.[4] The average viscosity of CMO and PUO was equivalent at $p \leq 0.05$ to the average viscosity of canola oil, which was observed to have the highest viscosity among the other edible oils assessed in the study. A study by Sahasrabudhe et al.[45] reported the average viscosity of canola oil to be lower than that of CMO and PUO. The high viscosity of the assessed oils in this study results from the high FFA composition in nonedible oils compared to edible oils.

3.4. The Influence of Temperature on Shear Stress and Viscosity. The influence of temperature on shear stress as a function of shear rate was analyzed at the temperatures of 30, 40, 50, and 60 °C. As expected, the results in Figure 3

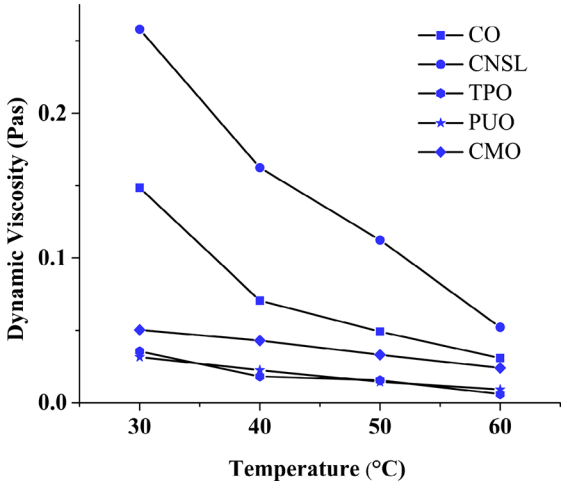

Figure 3. The variation of dynamic viscosity (Pa·s) with the increase in temperature.

revealed that, with an increase in temperature, the shear stress values exhibited by the samples decreased. The shear stress values of CNSL, CO, CMO, PUO, and TPO at the temperature of 30 °C and shear rate 100 s^{-1} were 16.95, 31.06, 3.76, 2.13, and 5.42 Pa, respectively. At 60 °C, the maximum shear stress values observed for CNSL, CO, CMO, PUO, and TPO were 4.25, 7.32, 1.20, 0.52, and 2.13 Pa, respectively. At the shear rate of 100 s^{-1}, the decrease in the shear stress from 30 to 60 °C was 74.5% for CNSL and CO, 31.9% for CMO, 24.4% for PUO, and 39.3% for TPO. Also, the viscosity of all the samples analyzed decreased as the temperature increased. The decrease in viscosity resulted in the low torque required to overcome the viscous resistance offered by the sample. This describes the decrease in shear stress, which resulted from the decrease of dynamic viscosity in the samples as the temperature increased. Figure 3 shows the effect of temperature on the dynamic viscosity of the samples. Drastic alterations of dynamic viscosity in CNSL and CO samples were observed as the temperature increased because the samples had carbon−carbon chains with a high unsaturation degree of FFA.[43] Unsaturated bonds were deformed under heat (temperature), bringing about drastic changes in the viscosity of the samples. Contrarily, the viscosity of CMO, PUO, and TPO steadily decreased, which implied that FFA bonds in the oil were not substantially deformed with the temperature increment. The results show that, regardless of the temperature variations, all samples maintained a constant linear flow behavior, with a constant viscosity resulting in a flow behavior index of approximately equal to 1 at 30, 40, 50, and 60 °C.

Since the viscosity of the samples was maintained at uniform temperatures, it is possible that the molecular structure and the molecular arrangement of the molecules were maintained as well throughout the experiments.[46] Newtonian fluids possess isotropic molecules that have a symmetrical shape, and the molecules are not oriented by the shear rate applied in the samples, therefore not causing any changes in the flow properties of the oils.[46] If the molecules are oriented by the force applied into the sample, dilatant or pseudoplastic flow of the samples would be observed. The molecules' orientation changes the direction of the molecular flow, resulting in the deviation of the direction of the shear stress. However, a comprehensive study on the microstructural changes resulting from shearing and temperature variations is recommended to examine their impacts on the sample's quality and the produced fuel.

However, as shown in Figure 4, the viscosity of PUO was comparatively similar to that of CMO. Likewise, as the

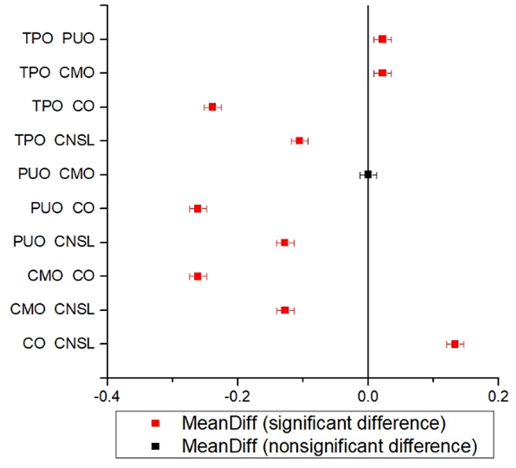

Figure 4. Mean dynamic viscosity comparison using Tukey's test.

temperature varied, the dynamic viscosity values comparison were still maintained. The Tukey test confirmed the resemblance in mean dynamic viscosity values at $p \leq 0.05$, as shown in Figure 4. The results suggested that the samples had equal internal resistance to flow, which could be contributed by the resemblance of the morphology of CMO

https://doi.org/10.1021/acsomega.2c02960
ACS Omega 2022, 7, 37133−37141

Table 7. Rheological Models' Parameters at 60 °C

	Newton $\tau = \eta\gamma$		Bingham $\tau = \tau_0 + \eta_p\gamma$			Ostwald–de Waele $\tau = K(\gamma)^n$			Herschel–Bulkley $\tau = \tau_0 + K(\gamma)^n$			
oils	η	R^2	τ_0	η_p	R^2	K	n	R^2	τ_0	K	n	R^2
CNSL	0.0355	0.997	−0.1141	0.0335	0.997	0.04695	0.932	1.000	0.0271	0.0435	0.9466	0.946
CO	0.0705	0.995	−0.3354	0.0750	0.997	0.03325	1.100	0.998	−0.0228	0.0347	1.146	0.943
CMO	0.0130	0.997	−0.0534	0.0137	0.981	0.01049	1.049	0.998	−0.1118	0.0248	0.8775	0.999
PUO	0.0150	1.000	−0.0150	0.0002	0.999	0.01520	0.9973	1.000	−0.0030	0.0156	0.9925	0.934
TPO	0.0208	1.000	0.00164	0.0208	0.956	0.02130	0.9950	1.000	−0.0045	0.0218	0.9899	1.000

and PUO. The similarities in morphology could include but are not limited to the inner structure, shape, arrangement, and size of the particles in the samples. Thus, the torque required to start the flow in CMO was equivalent to that of PUO. As a result, there was no significant difference in the shear stress exhibited at the respective shear rate for both CMO and PUO.

Moreover, according to power-law, the consistency index K, which describes the ease of flow for each sample, decreased as dynamic viscosity reduced. The computed data revealed that the consistency index fluctuated with the temperature increase, which decreased with an increase in temperature. Low consistency index values were observed at high temperatures, which suggested that the samples flow readily at high temperatures and vice versa. The computed consistency index values for each sample at 30, 40, 50, and 60 °C are presented in Tables 4–7.

3.5. Determination of the Appropriate Rheological Predictive Model for the Oils. Rheological models that could describe the flow behavior of the selected nonedible vegetable oils were assessed by fitting the experimental data into four rheological models selected. The models were the Newton, Bingham, Ostwald–de Waele (power-law), and Herschel–Bulkley rheological models. The selection of the models was on account of the time-independent behavior that was portrayed by the rheograms of the samples. The predictive models represented the shear stress–shear rate relationship by employing the introduction of flow predictive parameters in each model. The predictive flow parameters that were used for modeling are described in Tables 3–6.

In Newton's rheological model, the determinant predictive parameter was the apparent viscosity η (Pa·s). For all the samples, it was observed that the apparent viscosity was decreasing with the increase in temperature. As a result, it affected the shear stress (the study's dependent variable). The correlation coefficient calculated by the experimental data fitting into this rheological model was $R^2 \geq 0.987$. In Bingham's rheological model, the predictive parameters introduced in the shear rate–shear stress relationship were yield stress τ_0 (Pa) and Bingham's plastic viscosity η_p (Pa·s). Bingham's rheological model focused on the apparent viscosity of the samples at very low shear rates. The yield stress values exhibited by all the selected samples were $\tau_0 < 0$, which were not in correlation to the accepted values for the Bingham's fluids. The latter require yield stress greater than 0 ($\tau_0 > 0$) to initiate flow of the samples at the shear rate of 0 s^{-1}. The Bingham's plastic values for the samples were less than 0.5 Pa·s, resulting in negative yield stress values calculated. The correlation fit of the experimental data into this rheological model was $R^2 \geq 0.956$.

In Ostwald–de Waele's rheological model, the predictive parameters were consistency index K (Pa·s^n) and flow behavior index n. Irrespective of the characterization temperature, $n = 1$ and $K > 0$ for all the samples. The decrease of the consistency index with the increase in temperature revealed that the viscous resistance was weakened, resulting in oil thinning; hence, the pumping ability of the oils was increased. This observation would also be reflected in the manufactured biodiesel, which would mean that the quality of fuel atomization would be achieved at high temperatures. The computed predictive parameter values were correlated to the expected parameter values for the Ostwald–de Waele model, and a positive correlation was revealed. The experimental data fit in this model showed a correlation of $R^2 \geq 0.990$. The predictive parameters in the Herschel–Bulkley flow model were yield stress τ_0 (Pa), consistency index K (Pa·s^n), and flow behavior index n. The calculated yield stress values at 0 s^{-1} were $-0.7259 \leq \tau_0 \leq 0.0728$, which showed that the computed values were out of the expected range of $\tau_0 > 0$ for Herschel–Bulkley fluids. However, computed values for n and K were within the expected range for Herschel–Bulkley fluids, i.e., $0 < n < \infty$ and $K > 0$. The correlation of the fit in the Herschel–Bulkley model was $R^2 \geq 0.929$, which is not the most appropriate fit among the selected flow behavior predictive models.

According to the correlation coefficient (R^2) values computed by fitting the experimental data into the rheological models, the Newtonian, Ostwald–de Waele, and Bingham rheological models show an appropriate fit to describe the flow behavior of the samples. However, Herschel–Bulkley's model showed a weak correlation to the data. Also, some τ_0 values in Herschel–Bulkley's model were negative, which contrast with the expected yield stress of Herschel–Bulkley's model, $\tau_0 > 0$. Similarly, the computed yield stress values in the Bingham model were negative, meaning that none of the oils required externally applied stress to start flowing. Hence, Bingham's and Herschel–Bulkley's rheological models were not appropriate for presenting the flow behavior of the selected sample oils. The results of this study showed a resemblance to those of Paul et al.,[43] a study that analyzed the rheological characteristics of CO and methyl ester. Furthermore, the study reported that at low shear rates of 5–100 s^{-1}, CO and the manufactured methyl ester portrayed a non-Newtonian flow behavior. However, in this study, non-Newtonian flow behavior was not portrayed by any of the selected vegetable oils at the same shear rate. Additionally, a study by Abdelraziq and Nierat[47] showed that CO had a depicted Newtonian flow behavior irrespective of the shear rate and temperature at which the rheometer was operated. Therefore, all sample oils portrayed a Newtonian flow behavior, which was appropriately represented by Newton's and Ostwald–de Waele's rheological models. Research by Silva et al.[4] and Sahasrabudhe et al.[45] described that a similar flow behavior was exhibited by edible oils where the flow behavior index maintained was equal to 1 at elevated temperatures from 20 °C. The studies concluded that Newton's and Ostwald–de Waele's rheological models were

https://doi.org/10.1021/acsomega.2c02960
ACS Omega 2022, 7, 37133−37141

appropriate to present the flow behavior of the analyzed edible oils.

4. CONCLUSIONS

All the selected vegetable oils in this study had an oil yield of 29−65% from the seeds. The high oil yield shows that all the studied nonedible vegetable oils can be used to produce biodiesel commercially. However, the results revealed a significant difference in nonedible physical and chemical properties, solidifying the emphasis on the optimization of suitable designs of production facilities. Suitable designs should withstand the high viscous resistance offered by nonedible oils during the mixing process of raw materials. Rheological characterization revealed that, at a constant temperature, all selected nonedible vegetable oils exhibited a Newtonian flow behavior $n = 1$. All the sample oils used in this study maintained the same behavior at 30−60 °C. CNSL and CO had high viscosity among all the selected sample oils. In correspondence to their high viscosity nature, the produced biodiesel from CNSL and CO will perform poorly in cold climates. The high viscosity of CNSL and CO results in the increased cloud and pour points, which compromise the quality of fuel atomization. Though in-tank fuel heaters can resolve this issue, the method consumes enormous energy, which restricts the biodiesel's affordability aspect. A blend of high- and low-viscosity feedstock can counteract this challenge. However, research should be conducted to analyze the characteristics of a methyl ester of the produced oil blend and actual blend ratios. As expected, the temperature increase caused the decrease in viscosity and consistency index of the samples. The viscosity of CMO and PUO did not show any significant difference at the probability of $p \leq 0.05$. The rheological characteristics of the selected samples were appropriately represented by the Newtonian and Ostwald−de Waele rheological models. The rheological models showed a strong correlation to the fit of the experimental data (R^2 = 0.990−1.000). Therefore, for optimizing the biodiesel manufacturing process from nonedible oils, the average temperature for high-viscosity oils such as CSNL and CO should be maintained at 30−45 °C to avoid the irreversible deformation of the molecular structure of the produced biodiesel resulting in the compromise of the fuel's quality. However, for low-viscosity nonedible oils, there were no observed effects that could compromise the fuel's quality at the elevated temperatures. Correspondingly, the shear rate does not affect the oil's viscosity, ensuring the preservation of the fuel's quality through the production process. However, since the shear rate was directly proportional to the shear stress exhibited by the oils, the agitation speed to not exceed 800 rpm, to avert the damage on the manufacturing facilities from the exerted pressure. Manufacturing systems that can contain the high shear stress exerted by nonedible oils should as well be designed. Since this study focused solely on the flow behavior of the samples in relation to the production process, a further study on the microstructural interaction of the samples occurring because of the temperature and shear rate variations is recommended.

AUTHOR INFORMATION

Corresponding Author

Thomas Kivevele − *School of Materials, Energy, Water and Environmental Sciences (MEWES), The Nelson Mandela African Institution of Science and Technology (NM-AIST), Arusha 23118, Tanzania*; Email: thomas.kivevele@nm-aist.ac.tz

Authors

Francisca Zakaria − *School of Materials, Energy, Water and Environmental Sciences (MEWES), The Nelson Mandela African Institution of Science and Technology (NM-AIST), Arusha 23118, Tanzania*; orcid.org/0000-0003-0500-2358

Frank Lujaji − *Dar es Salaam Institute of Technology (DIT), Dar-es-salaam 367, Tanzania*

Complete contact information is available at: https://pubs.acs.org/10.1021/acsomega.2c02960

Author Contributions

All the authors contributed equally to this work, and the final version of the manuscript is approved by all the authors for submission.

Notes

The authors declare no competing financial interest.

ACKNOWLEDGMENTS

The authors acknowledge the support of the EXAF-JFD Project titled "Exploiting the potential of underutilized African plants and agricultural wastes in biofuels production" funded by Ecole Polytechnique Fédérale de Lausanne (EPFL), Switzerland, and Universite Mohammed VI Polytechnique (UM6P), Morocco. Also, the authors would like to express their sincere gratitude to The Nelson Mandela African Institution of Science and Technology, where the study was conducted.

NOMENCLATURE

CNSL − cashew nut shell liquid
CO − castor oil
CMO − *Croton megalocarpus* oil
PUO − *Podocarpus usambarensis* oil
TPO − *Thevetia peruviana* oil
K − consistency index
n − behavior index

REFERENCES

(1) Pinto, A. C.; Guarieiro, L. L.; Rezende, M. J.; Ribeiro, N. M.; Torres, E. A.; Lopes, W. A.; Pereira, P. A. d. P.; Andrade, J. B. d. Biodiesel: An Overview. *J. Braz. Chem. Soc.* **2005**, *16*, 1313−1330.

(2) Huang, D.; Zhou, H.; Lin, L. Biodiesel: An Alternative to Conventional Fuel. *Energy Procedia* **2012**, *16*, 1874−1885.

(3) Canakci, M.; Sanli, H. Biodiesel Production from Various Feedstocks and Their Effects on the Fuel Properties. *J. Ind. Microbiol. Biotechnol.* **2008**, *35*, 431−441.

(4) Silva, L. E.; Santos, C. A. C.; Ribeiro, J. E. S.; Souza, C. C.; Sant'Ana, A. M. S. Rheological Analysis of Vegetable Oils Used for Biodiesel Production in Brazil. *Rev. Eng. Term.* **2015**, *14*, 31−36.

(5) Ayoola, A. A.; Fayomi, O. S. I.; Adegbite, O. A.; Raji, O.Biodiesel Fuel Production Processes: A Short Review. In *IOP conference series: materials science and engineering*; IOP Publishing, 2021; Vol. *1107*, p 012151.

(6) Lin, L.; Cunshan, Z.; Vittayapadung, S.; Xiangqian, S.; Mingdong, D. Opportunities and Challenges for Biodiesel Fuel. *Appl. Energy* **2011**, *88*, 1020−1031.

(7) Supriyanto, E.; Sentanuhady, J.; Dwiputra, A.; Permana, A.; Muflikhun, M. A. The Recent Progress of Natural Sources and Manufacturing Process of Biodiesel: A Review. *Sustainability* **2021**, *13*, 5599.

https://doi.org/10.1021/acsomega.2c02960
ACS Omega 2022, 7, 37133−37141

(8) Gandhi, T.; Patel, M.; Dholakiya, B. K. Studies on Effect of Various Solvents on Extraction of Cashew Nut Shell Liquid (CNSL) and Isolation of Major Phenolic Constituents from Extracted CNSL. *J. Nat. Prod. Plant Resour.* **2012**, *2*, 135−142.
(9) Kyei, S. K.; Akaranta, O.; Darko, G.; Chukwu, U. J. Extraction, Characterization and Application of Cashew Nut Shell Liquid from Cashew Nut Shells. *Chem. Sci. Int. J.* **2019**, 1−10.
(10) Aliyu, B.; Agnew, B.; Douglas, S. Croton Megalocarpus (Musine) Seeds as a Potential Source of Bio-Diesel. *Biomass Bioenergy* **2010**, *34*, 1495−1499.
(11) Román-Figueroa, C.; Cea, M.; Paneque, M.; González, M. E. Oil Content and Fatty Acid Composition in Castor Bean Naturalized Accessions under Mediterranean Conditions in Chile. *Agronomy* **2020**, *10*, 1145.
(12) Bora, M. M.; Gogoi, P.; Deka, D. C.; Kakati, D. K. Synthesis and Characterization of Yellow Oleander (Thevetia Peruviana) Seed Oil-Based Alkyd Resin. *Ind. Crops Prod.* **2014**, *52*, 721−728.
(13) Minzangi, K.; Kaaya, A. N.; Kansiime, F.; Tabuti, J. R. S.; Samvura, B. Oil Content and Physicochemical Characteristics of Some Wild Oilseed Plants from Kivu Region Eastern Democratic Republic of Congo. *Afr. J. Biotechnol.* **2011**, *10*, 189−195.
(14) Kibazohi, O.; Sangwan, R. S. Vegetable Oil Production Potential from Jatropha Curcas, Croton Megalocarpus, Aleurites Moluccana, Moringa Oleifera and Pachira Glabra: Assessment of Renewable Energy Resources for Bio-Energy Production in Africa. *Biomass Bioenergy* **2011**, *35*, 1352−1356.
(15) Temitayo, O. D. Optimization of Oil Extraction from Thevetia Peruviana (Yellow Oleander) Seeds: A Case Study of Two Statistical Models. *Int. J. Eng. Mod. Technol.* **2017**, *3*, 2504−8856.
(16) Aga, W. S.; Fantaye, S. K.; Jabasingh, S. A. Biodiesel Production from Ethiopian 'Besana'- Croton Macrostachyus Seed: Characterization and Optimization. *Renewable Energy* **2020**, *157*, 574−584.
(17) Yadav, A. K.; Khan, M. E.; Pal, A.; Dubey, A. M. Biodiesel Production from Nerium Oleander (Thevetia Peruviana) Oil through Conventional and Ultrasonic Irradiation Methods. *Energy Sources, Part A* **2016**, *38*, 3447−3452.
(18) Dhoot, S. B.; Jaju, D. R.; Deshmukh, S. A.; Panchal, B. M.; Sharma, M. R. Extraction of Thevetia Peruviana Seed Oil and Optimization of Biodiesel Production Using Alkalicatalyzed Methanolysis. *J. Alternate Energy Sources Technol.* **2011**, *2*, 8−16.
(19) Suwari; Kotta, H. Z.; Buang, Y.Optimization of Soxhlet Extraction and Physicochemical Analysis of Crop Oil from Seed Kernel of Feun Kase (*Thevetia Peruviana*). In *AIP Conference Proceedings*; AIP Publishing LLC, 2017; Vol. *1911*, p 020005.
(20) Mezger, T.*Rheology Handbook, Hannover: William Andrew*; AppliedSci Publishers, 2012.
(21) Mezger, T.*The Rheology Handbook*; Vincentz Network, 2020.
(22) Schramm, G.*A Practical Approach to Rheology and Rheometry*; Haake Karlsruhe, 1994.
(23) Annongu, A. A.; Joseph, J. K. Proximate Analysis of Castor Seeds and Cake. *J. Appl. Sci. Environ. Manage.* **2008**, *12*, 39.
(24) Olatunji, O. M.; Akor, A. J.; Akintayo, C. O. Analysis of Some Physio-Chemical Properties of Milk Bush (*Thevetia Peruviana*) Seeds. *Res. J. Appl. Sci., Eng. Technol.* **2011**, *10*, 84.
(25) Rodrigues, F. H. A.; França, F. C. F.; Souza, J. R. R.; Ricardo, N. M. P. S.; Feitosa, J. P. A. Comparison between Physico-Chemical Properties of the Technical Cashew Nut Shell Liquid (CNSL) and Those Natural Extracted from Solvent and Pressing. *Polímeros* **2011**, *21*, 156−160.
(26) Suraj, C. K.; Anand, K.; Sundararajan, T. Investigation of Biodiesel Production Methods by Altering Free Fatty Acid Content in Vegetable Oils. *Biofuels* **2020**, *11*, 587−595.
(27) Bouaid, A.; Vázquez, R.; Martinez, M.; Aracil, J. Effect of Free Fatty Acids Contents on Biodiesel Quality. Pilot Plant Studies. *Fuel* **2016**, *174*, 54−62.
(28) Udoh, J.; Olayanju, T.; Dairo, O. Akindele Alonge. Effect of Moisture Content on the Mechanical and Oil Properties of Soursop Seeds. *Chem. Eng. Trans.* **2017**, *58*, 361−366.
(29) Kivevele, T. T.; Mbarawa, M. M. Comprehensive Analysis of Fuel Properties of Biodiesel from Croton Megalocarpus Oil. *Energy Fuels* **2010**, *24*, 6151−6155.
(30) Uwiragiye, B.; Anyiam, P. Phytochemical Screening and Physicochemical Properties of Oil and Biodiesel Produced from Non-Edible Croton Megalocarpus Seeds Grown in Huye District. *GSJ* **2020**, *8*, 2505.
(31) Omari, A.; Mgani, Q. A.; Mubofu, E. B. Fatty Acid Profile and Physico-Chemical Parameters of Castor Oils in Tanzania. *Green Sustainable Chem.* **2015**, *05*, 154−163.
(32) Chavan, M.; Sutar, A.; Bhatkande, R.; Gurav, R.; Mulla, M.; Deokar, A.; Harari, P. Experimental Studies on Production of Biodiesel from *Thevetia Peruviana* Feedstock. *Int. J. Eng. Manage. Res.* **2018**, *8*, 46.
(33) Shaah, M. A. H.; Hossain, M. S.; Allafi, F. A. S.; Alsaedi, A.; Ismail, N.; Ab Kadir, M. O.; Ahmad, M. I. A Review on Non-Edible Oil as a Potential Feedstock for Biodiesel: Physicochemical Properties and Production Technologies. *RSC Adv.* **2021**, *11*, 25018−25037.
(34) Shalaby, E. A. A Review of Selected Non-Edible Biomass Sources as Feedstock for Biodiesel Production. *Biofuels* **2015**, 3−20.
(35) Kumar, A.; Chirchir, A.; Namango, S.; Kiriamiti, H.Microwave Irradiated Transesterification of *Croton Megalocarpus* Oil−Process Optimization Using Response Surface Methodology. In *Proceedings of Sustainable Research and Innovation Conference*; 2016; pp. 132−137.
(36) Patterson, H. B. W.Quality and Control. In *Hydrogenation of fats and oils*; Elsevier, 2011; pp. 329−350, DOI: 10.1016/B978-1-893997-93-6.50018-X.
(37) Eke, W. I.; Achugasim, O.; Ofordile, S. E.; Ajienka, J.; Akaranta, O.Performance Evaluation of Cashew Nut Shell Liquid CNSL as Flow Improver for Waxy Crude Oils. In *SPE Nigeria Annual International Conference and Exhibition*; OnePetro, 2019.
(38) Iqbal, J.; Martin, S.; Carney, Jr., W.*Feedstock Quality Issues for Biodiesel Production*; Google Search, 2011.
(39) Ana Godson, R. E. E.; Udofia Bassey, G. Characterization of Oil and Biodiesel Produced from Thevetia Peruviana (Yellow Oleander) Seeds. *Int. J. Sustainable Green Energy* **2015**, *4*, 150−158.
(40) Wu, D.; Roskilly, A. P.; Yu, H. Croton Megalocarpus Oil-Fired Micro-Trigeneration Prototype for Remote and Self-Contained Applications: Experimental Assessment of Its Performance and Gaseous and Particulate Emissions. *Interface Focus* **2013**, *3*, 20120041.
(41) Karmakar, B.; Halder, G. Progress and Future of Biodiesel Synthesis: Advancements in Oil Extraction and Conversion Technologies. *Energy Convers. Manage.* **2019**, *182*, 307−339.
(42) Zulqarnain; Ayoub, M.; Yusoff, M. H. M.; Nazir, M. H.; Zahid, I.; Ameen, M.; Sher, F.; Floresyona, D.; Budi Nursanto, E. A Comprehensive Review on Oil Extraction and Biodiesel Production Technologies. *Sustainability* **2021**, *13*, 788.
(43) Paul, A. K.; Borugadda, V. B.; Reshad, A. S.; Bhalerao, M. S.; Tiwari, P.; Goud, V. V. Comparative Study of Physicochemical and Rheological Property of Waste Cooking Oil, Castor Oil, Rubber Seed Oil, Their Methyl Esters and Blends with Mineral Diesel Fuel. *Mater. Sci. Energy Technol.* **2021**, *4*, 148−155.
(44) Wang, H.; Qian, S.; Ni, Z.; Huang, C.; Zhao, Y. Experimental Investigation on the Rheological Properties of Castor Oil at Different Temperatures. *Proc. Inst. Mech. Eng., Part J* **2018**, *232*, 861−870.
(45) Sahasrabudhe, S. N.; Rodriguez-Martinez, V.; O'Meara, M.; Farkas, B. E. Density, Viscosity, and Surface Tension of Five Vegetable Oils at Elevated Temperatures: Measurement and Modeling. *Int. J. Food Prop.* **2017**, *20*, 1965−1981.
(46) RheoSense Inc.*Viscosity of Newtonian and Non-Newtonian Fluids*;https://www.rheosense.com/applications/viscosity/newtonian-non-newtonian (accessed 2022-08-29).
(47) Abdelraziq, I. R.; Nierat, T. H. Rheology Properties of Castor Oil: Temperature and Shear Rate-Dependence of Castor Oil Shear Stress. *J. Mater. Sci. Eng.* **2015**, *5*, 1000220.

https://doi.org/10.1021/acsomega.2c02960
ACS Omega 2022, 7, 37133−37141